Improving the Four-Dimensional Incremental Analysis Update (4DIAU) with the HWRF 4DEnVar Data Assimilation System for Rapidly Evolving Hurricane Prediction

XU LU[a] AND XUGUANG WANG[a]

[a] *School of Meteorology, University of Oklahoma, Norman, Oklahoma*

(Manuscript received 1 April 2021, in final form 20 August 2021)

ABSTRACT: Short-term spinup for strong storms is a known difficulty for the operational Hurricane Weather Research and Forecasting (HWRF) Model after assimilating high-resolution inner-core observations. Our previous study associated this short-term intensity prediction issue with the incompatibility between the HWRF Model and the data assimilation (DA) analysis. While improving physics and resolution of the model was found to be helpful, this study focuses on further improving the intensity predictions through the four-dimensional incremental analysis update (4DIAU). In the traditional 4DIAU, increments are predetermined by subtracting background forecasts from analyses. Such predetermined increments implicitly require linear evolution assumption during the update, which are hardly valid for rapidly evolving hurricanes. To confirm the hypothesis, a corresponding 4D analysis nudging (4DAN) method, which uses online increments is first compared with the 4DIAU in an oscillation model. Then, variants of 4DIAU are proposed to improve its application for nonlinear systems. Next, 4DIAU, 4DAN and their proposed improvements are implemented into the HWRF 4DEnVar DA system and are investigated with Hurricane Patricia (2015). Results from both the oscillation model and HWRF Model show that 1) the predetermined increments in 4DIAU can be detrimental when there are discrepancies between the updated and background forecasts during a nonlinear evolution; 2) 4DAN can improve the performance of incremental update upon 4DIAU, but its improvements are limited by the overfiltering; 3) relocating initial background before the incremental update can improve the corresponding traditional methods; and 4) the feature-relative 4DIAU method improves the incremental update the most and produces the best track and intensity predictions for Patricia among all experiments.

KEYWORDS: Hurricanes; Data assimilation; Model initialization; Numerical weather prediction/forecasting

1. Introduction

An increasing number of types of observations have been made available to provide a better understanding of the dynamics and thermodynamics of the inner-core region of the tropical cyclones (TC) (Lu and Wang 2020). To better utilize these emerging observations in a numerical weather prediction (NWP) system, an advanced data assimilation (DA) approach is needed. In the past few decades, ensemble-based DA approaches such as the ensemble Kalman filter (EnKF) and the ensemble–variational (EnVar) methods have been widely used for TC predictions and have shown promising improvements in both track and intensity predictions after assimilating the inner-core observations (Torn and Hakim 2009; Xiao et al. 2009; Zhang et al. 2009, 2011; Li et al. 2012; Weng and Zhang 2012; Aksoy et al. 2013; Lu et al. 2017a,b; Lu and Wang 2019).

However, advanced inner-core DA is not always improving the hurricane predictions. For example, the operational Hurricane Weather Research and Forecasting (HWRF) Model has difficulties in spinning up the short-term surface wind maximum (Vmax) after assimilating high-resolution inner-core observations, which degrades its short-term intensity predictions for strong storms (Tong et al. 2018). While early studies attributed the issue to the inferior initial analysis (Bernardet et al. 2015; Zhou et al. 2015; Pu et al. 2016), Lu and Wang (2019) found that such a short-term Vmax degradation is likely a result of the incompatibility between the HWRF Model and DA analysis. For example, when the storm structure from an advanced inner-core DA analysis better emulates the reality, the model with less realistic physics cannot support and therefore requires longer time to adjust to the analyzed TC. While improving the model physics was found to alleviate the issue and improve the intensity predictions according to Lu and Wang (2019), the mismatch between model and DA analysis inevitably exists. This current study aims at further improving the TC intensity predictions by updating the model through using the DA analysis incrementally.

Early studies suggested that intermittent DA updates can introduce noises or imbalances into the NWP models (Morel and Talagrand 1974; Hoke and Anthes 1976; Harms et al. 1992). These undesired features, which are usually identified as shocks to the surface pressure tendency evolution (Lynch and Huang 1992), may be developed into spurious gravity waves, and can induce detrimental initialization or spinup problems for the NWP models (Lee et al. 2006; Benkiran and Greiner 2008). Lots of methods have been proposed to mollify this initialization concern since last century, such as nudging or Newtonian relaxation (Hoke and Anthes 1976), the normal mode initialization (Machenhauer 1977; Daley 1978), digital filtering (Lynch and Huang 1992; Huang and Lynch 1993), and the incremental analysis update (IAU) (Bloom et al. 1996).

IAU is one of the most widely used methods to address the spinup concerns for the NWP models (Macpherson 2001; Zhu et al. 2003; Lee et al. 2006; Zuo et al. 2019; Heng et al. 2020). Instead of adding the DA analysis increment intermittently to the model fields with dramatic changes at once, IAU uses the

Corresponding author: Xuguang Wang, xuguang.wang@ou.edu

DOI: 10.1175/MWR-D-21-0068.1

increment as an additional but continuous forcing to the model integration (Bloom et al. 1996). The continuous but relatively small forcing added to each model integration time step is designed to maximally maintain the dynamical balance of the mass and momentum fields of the model, and therefore reduce the shocks caused by the intermittent DA. Early IAU methods include the three-dimensional (3D) approach (3DIAU), which considered one single 3D analysis increment without accounting for the incremental propagation within the DA time window (Bloom et al. 1996). A four-dimensional IAU (4DIAU) was later proposed to account for 4D analysis increment (Lorenc et al. 2015) and was found to significantly reduce the model spinup as compared to the corresponding digital filter method (Buehner et al. 2015). The 4DIAU method has been implemented by many operational centers, such as the Met Office (Lorenc et al. 2015), the Environmental Canada global deterministic prediction system (Buehner et al. 2015), and the National Centers for Environmental Prediction (NCEP; Lei and Whitaker 2016). But to the best knowledge of the authors, the 4DIAU has not been examined in a regional convection allowing model like HWRF where fast evolving meso- and convective-scale weather system like hurricanes are simulated.

In the traditional 4DIAU, increments are predetermined by subtracting the background forecasts from the 4D analyses. Then these predetermined increments are incrementally added to the model forecasts as external forcing to the model. An implicit assumption of this approach is that the systems are linear or near-linear so that the updated model status would remain unchanged or perform similarly to the background forecasts. For the highly nonlinear and rapidly changing weather systems like hurricanes, this assumption is easily violated. The predetermined analysis increments can be added to the wrong places or phases, which can cause detrimental issues to the subsequent forecast. Therefore, improvement of the 4DIAU method is needed before applying the 4DIAU to regional hurricane analysis and prediction system. Two variants of the 4DIAU method are proposed and investigated in this study.

Analysis nudging (AN) is another incremental approach that gradually inserts the DA analysis into the model integration through an additional model forcing term. Unlike IAU, AN "nudges" the model predictions toward the DA analyses using differences between the model prediction and the DA analysis determined online instead of using the predetermined analysis increments. By doing so, AN would additionally filter the background state while the IAU only filters the analysis increment (Bloom et al. 1996; Bao and Errico 1997). This extra filtering on the background state is undesirable as it was found to remove features like the diurnal or tidal signals. But in the meantime, concerns from the predetermined increments in 4DIAU are also no longer valid for 4DAN. Thus, in this study, 4DAN is also investigated and compared with the 4DIAU and its variants to confirm our hypotheses about the issues of 4DIAU.

Patricia (2015) was a record-breaking category-5 hurricane whose rapid intensification (RI) and peak intensity was not captured by most operational centers at the time (Rogers et al. 2017; Qin and Zhang 2018). To be more specific, in this 5-day hurricane with a small size, Patricia started its extraordinary RI from 0600 UTC 21 October to 0600 UTC 23 October. Its Vmax change was from about 18 to 95 m s^{-1} within 48 h, while the traditional definition of an RI is just 18 m s^{-1} within 24 h (Kaplan et al. 2010). Meanwhile, the hurricane was sampled by multiple field campaigns simultaneously, such as the Intensity Forecasting Experiment (IFEX) project (Rogers et al. 2006, 2013), and the Tropical Cyclone Intensity (TCI) project (Doyle et al. 2017). Those field campaign observations together with the "enhanced" atmospheric motion vector (AMV) observations from the Cooperative Institute for Meteorological Satellite Studies (CIMSS) (Wu et al. 2015; Velden et al. 2017) provided rarely abundant 3D observations to sample the inner-core, the upper-level outflow, the low-level inflow and the environment flow (Lu and Wang 2020). The extremely detailed sampling and the rapidly changing evolution of Patricia makes it a very good case to investigate the impact of various incremental update methods on the TC intensity predictions in a highly nonlinear situation. More details about the data and their impacts on DA analysis can be found in (Lu and Wang 2020).

The ultimate goal of this study is to improve the 4DIAU methods for the short-term intensity prediction of hurricanes. To achieve the goal, several scientific questions are being addressed in this study: (i) What are the issues or limitations of applying 4DIAU in the rapidly evolving hurricane predictions? (ii) How does 4DIAU compare with 4DAN in rapidly evolving hurricane cases? (iii) What are the benefits and limitation of the proposed 4DIAU variants in real case applications?

In this manuscript, we first use an idealized framework to illustrate the methodology of 4DIAU, its issue, and the proposed improvements in section 2. The methodology of 4DAN is also elucidated and compared with 4DIAU in the same framework in section 2. The HWRF Model, the observations and experiment designs for Hurricane Patricia are described in section 3. Section 4 shows the results of the impacts of the various incremental update methods on Patricia predictions. Section 5 concludes and further discusses the paper.

2. Improving 4DIAU in an idealized oscillation model

a. Methodology and idealized results of traditional 4DIAU

This subsection describes the general methodology of 4DIAU. Following (Lei and Whitaker 2016), to facilitate the understanding, a simple oscillation model is adopted in this section. For consistency, some equations and description mirror those from Lei and Whitaker (2016) with adaptions. The truth state at time t is given by

$$f^T(x,t) = A\cos(k_T x - \omega_T t), \tag{1}$$

where A, k_T, and ω_T are constants of the truth for amplitude, wavenumber, and angular frequency, respectively. The model state is given by

$$f^M(x,t) = B\cos(k_M x - \omega_M t + t_{\mathrm{PE}}), \tag{2}$$

where B, k_M, ω_M, and t_{PE} are constants of the model for amplitude, wavenumber, angular frequency, and phase error,

respectively. Assuming we can produce a perfect analysis state $f^a(x, t) = f^T(x, t)$, and the analysis increment at time t is

$$\Delta f(x,t) = f^T(x,t) - f^M(x,t). \tag{3}$$

Considering the increments from the nearest analysis times t_0 and t_1, the individual 4DIAU forcing added to the model integration as an external forcing term at time t (where $t_0 < t < t_1$) is set to

$$\Delta f(x,t)_{\text{4DIAU}} = \frac{w_1 \Delta f(x,t_0) + w_2 \Delta f(x,t_1)}{(N-1)(t_1 - t_0)}, \tag{4}$$

where $w_1 = (t_1 - t)/(t_1 - t_0)$, $w_2 = (t - t_0)/(t_1 - t_0)$, and N is the total number of increments during the time window.

Using the trapezoidal rule approximation following Lei and Whitaker (2016), the corresponding total integral of the 4DIAU forcing at the end of an assimilation window $[t_c - (\tau/2), t_c + (\tau/2)]$ is therefore

$$\int_{t_c-(\tau/2)}^{t_c+(\tau/2)} \Delta f(x)_{\text{4DIAU}} = \sum_{j=1}^{N-1} \frac{\Delta f\left(x, t_c - \frac{\tau}{2} + \frac{j-1}{N-1}\tau\right) + \Delta f\left(x, t_c - \frac{\tau}{2} + \frac{j}{N-1}\tau\right)}{2(N-1)}, \tag{5}$$

where τ is the DA time window length, and t_c is the center of the time window.

To help better visualize the effect of 4DIAU, a single wave evolution for the background model forecast and the truth is first plotted as blue and black solid lines in Figs. 1a–1e, respectively. The wave configurations follow Eqs. (1) and (2), and the parameters are set to $A = 3$; $B = 2$; $k_T = 1$; $k_M = 0.7$; $\omega_T = 1$; $\omega_M = 1$; and $t_{\text{pe}} = -\pi/2$ to mimic the real case situation in section 4. Specifically, the amplitude, wavelength, phase and speed differences in this idealized case roughly correspond to the intensity, size, location and motion differences of the storms produced by the HWRF background forecast and the 4DEnVar analysis, respectively. For simplification, the evolution is from phase $-\pi/2$ to phase $\pi/2$ and only five increments are considered every $\pi/4$, and the idealized 4DIAU-enabled prediction (4DIAU-Ideal) is shown in dashed purple lines in Figs. 1a–1e using Eqs. (3)–(5). In this idealized case, the 4DIAU-Ideal forecast moves at the same speed as the background model during the updates, which is $v_M = \omega_M/k_M \sim 1.42$. As shown in Fig. 1p, the final 4DIAU-Ideal analysis differs from the truth. But in general, the final wave pattern of the 4DIAU-Ideal is reasonably more consistent with the truth as compared to the background despite slight phase error, a little amplitude loss and small errors in the tails.

b. *Implicit linear assumption issue of traditional 4DIAU*

Although the performance of 4DIAU-Ideal is reasonable as shown in section 2a, its evolution requires that the updated forecasts remain the same moving speed as the background forecast. Such an implicit assumption may be reasonable for a linear or near-linear system, but is not valid for a rapidly changing nonlinear system. During the incremental update of a nonlinear system, the modified wave will naturally move slower from $v_M = 1.42$ toward $v_T = \omega_T/k_T = 1$ as it becomes more alike the truth. To simplify the situation, we assume a constant moving speed of $v_c \sim 1.23$ ($v_T < v_c < v_M$) for the updated forecasts to represent the speed discrepancy during the process, and the corresponding 4DIAU evolution is shown in Figs. 1f–1j. Clearly, when the phase of the updated forecast $f^{\text{4DIAU}}(x, t)$ drifts away from the background forecast $f^M(x, t)$, the predetermined increments calculated from Eq. (3) will be added to wrong places and result in detrimental discontinuities or spikes to the modified wave such as the sharp jumps around 1.2π and 4π (Figs. 1h–j).

In contrast to the 4DIAU, the 4DAN method does not predetermine the increments. Instead, the additional forcing term is adaptively calculated using online differences between the current model forecasts and the analyses. Thus, 4DAN suffers less from the linear assumptions than 4DIAU. To be consistent with and as an analogy to 4DIAU, the external 4DAN forcing term added to the model integration at time step t (where $t_0 < t < t_1$) is defined as

$$\Delta f(x,t)_{\text{4DAN}} = \frac{w_1[f^T(x,t_2) - f^{\text{4DAN}}(x,t)] + w_2[f^T(x,t_1) - f^{\text{4DAN}}(x,t)]}{(N-1)}, \tag{6}$$

where the weighting coefficients w_1 and w_2 are defined the same way as in Eq. (4), and $f^{\text{4DAN}}(x, t)$ is the current model forecast at time t.

The evolution of 4DAN is shown in Figs. 1k–1o. The figures show that the disruptive effects in both the main body and tail regions of the wave in 4DAN are much less as compared to those in 4DIAU (Fig. 1p). This result confirms the hypothesis that the implicit linear requirement when using the predetermined increments is indeed one major error source for nonlinear applications in 4DIAU. However, the amplitude error from the final 4DAN forecast is also larger than that of 4DIAU. The issue is likely due to the larger filtering effect in 4DAN which not only filters the analysis increments, but also filters the background.

c. *Removing initial phase error before the incremental update*

In this simple oscillation model, primary differences between the model background and the truth are from the phase, amplitude, and wavelength. Sensitivity experiments suggest that the phase difference contributes significantly more than the other two (the evolution of the wave after removing wavelength and

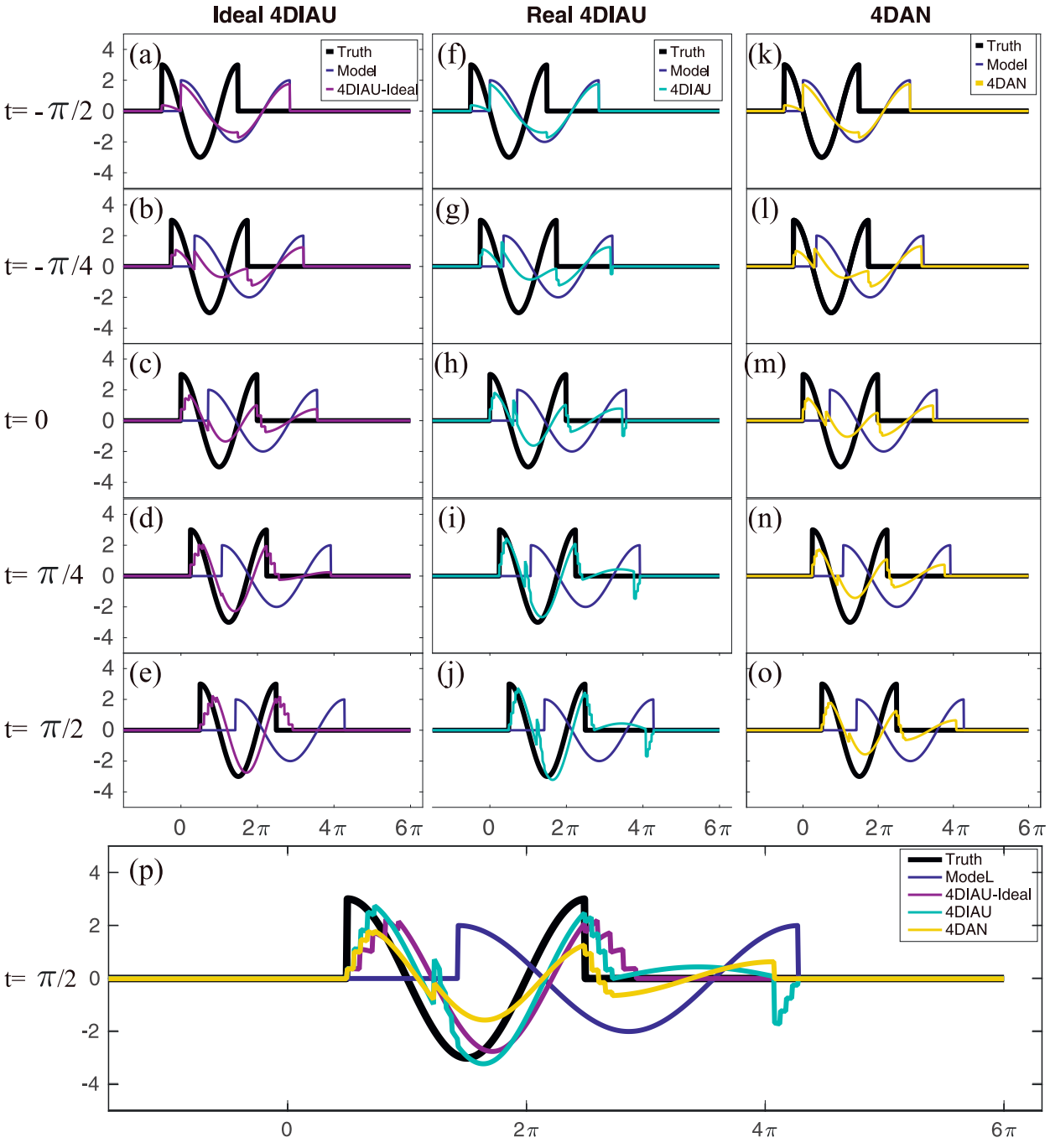

FIG. 1. Evolution of a simple oscillation model for the truth (black), background model (blue), and (a)–(e) idealized 4DIAU (purple), (f)–(j) 4DIAU (cyan), and (k)–(o) 4DAN (gold) from $-\pi/2$ to $\pi/2$. (p) The final forecasts of each experiment are shown together for comparison.

amplitude error is similar to Figs. 1f–1j, not shown) to the spikes in 4DIAU when the moving speed discrepancy exists.

Therefore, in experiment 4DIAU-RL, we propose to relocate the background model forecast to the truth location before 4DIAU (Fig. 2a). Such a removal of initial phase error in 4DIAU-RL produces a significant improvement during the incremental update according to Figs. 2a–2e. For example, the main body of the wave in 4DIAU-RL was intact, and the final phase error is also reduced compared to 4DIAU. Yet, Fig. 2p indicates that 4DIAU-RL can still have large discontinuities in the tails of the wave, which disagree with the truth.

Correspondingly, experiment 4DAN-RL is conducted by removing initial phase error prior to 4DAN. Figures 2f–2j show that the evolution of 4DAN-RL is also much more improved

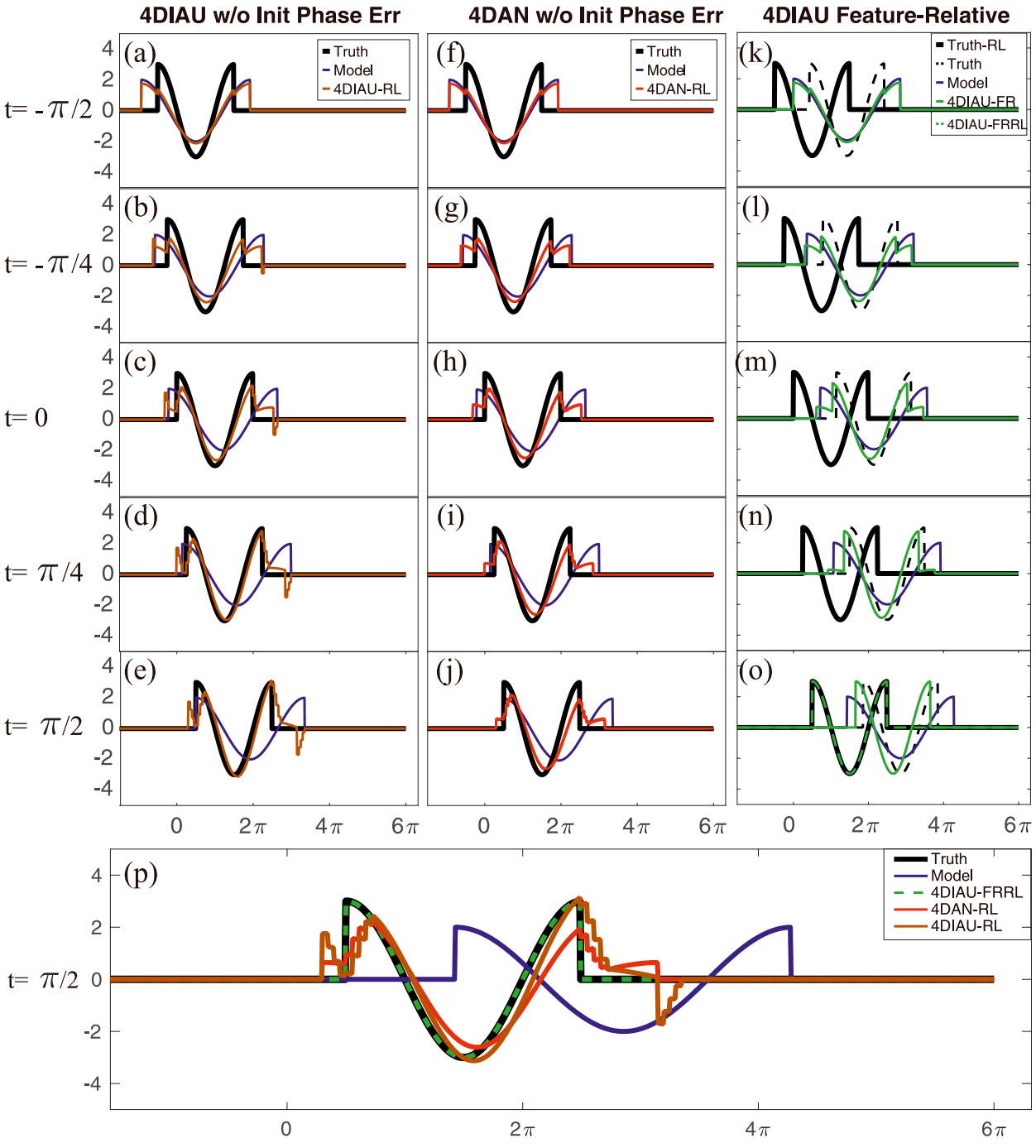

FIG. 2. As in Fig. 1, but for (a)–(e) 4DIAU-RL (brown), (f)–(j) 4DAN-RL (red), and (k)–(o) 4DIAU-FR (green). The final forecast of 4DIAU-FR (4DIAU-FRRL) will be relocated to the truth location and is shown as green dashes in (o).

upon 4DAN with its final forecast matches the truth better (Fig. 2p). For example, the amplitude error is becoming much smaller in 4DAN-RL. The improvement is likely due to the smaller total differences between the model background and the analysis. However, overfiltering effect still exists as the amplitude of the final wave is still smaller than both 4DIAU-RL and the truth.

Comparisons between 4DIAU and 4DIAU-RL, and 4DAN and 4DAN-RL demonstrate that the initial phase error can be a large error source for both incremental update methods (Fig. 1p vs Fig. 2p). And the comparison between 4DAN-RL and 4DIAU-RL also further confirms the hypothesis that using the predetermined increments in nonlinear evolutions is a major concern for the 4DIAU methods, especially when the

TABLE 1. List of observations assimilated.

Conventional in situ observations in prepbufr		Radiosondes
		Dropwindsondes
		Aircraft reports
		Surface ship and buoy observations
		Surface observations over land
		Pibal winds
		Wind profilers
		Radar-derived velocity azimuth display wind
		WindSat scatterometer winds
		Integrated precipitable water derived from the global positioning system
Airborne observations on board NOAA WP-3D aircraft from HFIP		Tail Doppler radar radial velocity
		Stepped Frequency Microwave Radiometer (SFMR)
		Flight-level wind, temperature, and specific humidity observations
High Definition Sounding System (HDSS) dropsodes from the TCI program		
MSLP from TCVital		
Enhanced atmospheric motion vectors from the CIMSS		
Satellite radiances	IR	HIRS
		AIRS
		IASI
		GOES
	MW	AMSU-A
		MHS
		ATMS

moving speed discrepancy between the updated and background forecasts exists (Fig. 2p).

d. Improving 4DIAU with feature-relative approach

As discussed in the previous sections, a major concern of the 4DIAU methods is the moving speed discrepancy between the updated and background forecasts, which is the primary contribution to the degraded 4DIAU forecast. Thus, one feature-relative 4DIAU (4DIAU-FR) approach is proposed in this subsection to address the issue.

In this 4DIAU-FR method, predetermined increments are calculated relative to the features (e.g., wave in this case, or storm in the hurricane case) by collocating the 4DEnVar analyzed wave (storm) with the background wave (storm; e.g., Truth-RL in Figs. 2k–o). Then, during the incremental update step, the increments are added only relative to the wave (storm). In other words, these feature-relative predetermined increments are only correcting the structure of the wave (storm) and are not correcting the phase (location) error. After all the structural modifications are added, the phase (location) error is accounted by relocating the final forecast to the analyzed position. This way, the 4DIAU-FR method is split into two parts: part one modifies the wave (storm) structures incrementally, and part two corrects the phase (location) error.

Figures 2k–2o show that the 4DIAU-FR can produce a final analysis that is very consistent with the truth, which has a RMSE of almost zero using the simplified model. This result again confirms the earlier results that if left untreated the speed discrepancy between the updated and background forecasts as a result of nonlinear evolution in the DA window can degrade the 4DIAU result. The proposed 4DIAU-FR approach shows potential to improve 4DIAU in the nonlinear situations.

3. Model, data, and experiment design

a. Model and observation descriptions

The 4DIAU and 4DAN capabilities are implemented into the newly developed dual-resolution, hybrid 4DEnVar DA system for HWRF (Lu et al. 2017a,b) using Eqs. (1)–(6) in section 2. Following Lu and Wang (2019), the horizontal grid spacing of the model is approximately 0.67 km (0.005°), 2 km (0.015°), and 6 km (0.045°) for the innermost (529 × 940 grid points), intermediate (265 × 472 grid points), and outermost (268 × 568 grid points) domains, respectively. The model has 61 vertical levels with its top at 2 hPa. The Ferrier–Aligo microphysics scheme (Tallapragada et al. 2015), simplified Arakawa–Schubert (SAS) cumulus scheme (Grell 1993; Hong and Pan 1996; Han and Pan 2011), HWRF surface layer scheme (Tallapragada et al. 2015), Noah land surface model (LSM) (Ek et al. 2003), the nonlocal hybrid eddy-diffusivity mass-flux (hybrid EDMF) PBL scheme (Hong and Pan 1996; Han et al. 2016), and RRTMG longwave and shortwave radiation schemes (Iacono et al. 2008) are used to parameterize the microphysics, cumulus, surface layer, land surface, planetary boundary layer and radiation processes, respectively. The vertical and horizontal diffusion in the PBL scheme is modified following Lu and Wang (2019). Specifically, a fix in the vertical turbulent diffusion profile is added to enable the in-cloud mixing for the deep convection regions like the eyewall or rainbands following (Zhu et al. 2019). And the horizontal diffusion is reduced to be consistent with the model resolution increase following (Zhang et al. 2018). These model physics and resolution configurations are from Lu and Wang (2019). As discussed in Lu and Wang (2019), the modified suite of model physics and resolution is to produce a better intensity prediction that best utilizes the advanced inner-core DA

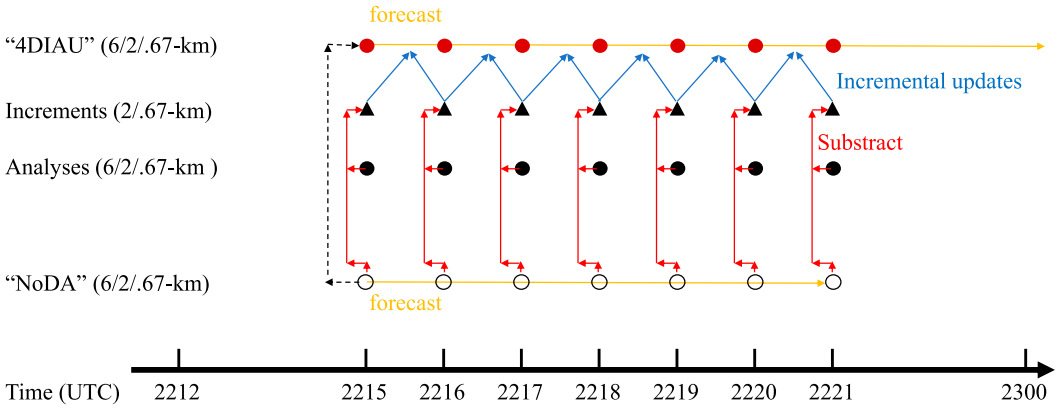

FIG. 3. Flowchart for experiment 4DIAU. Circles are the free forecast initialized from the previous DA cycle valid at 1200 UTC. Black dots are the 4DEnVar analyses. Triangles are the predetermined increments from the differences between NoDA (circle) and 4DEnVar analyses (black dots). The red dots are 4DIAU forecasts with the updates from the predetermined increments (triangles).

analysis. Sensitivity experiments show that the conclusions about IAU using the unmodified physics and resolution are generally qualitatively consistent with the conclusions shown in this study (not shown).

The observations assimilated in this study are listed in Table 1. Briefly, these are the observations from multiple field campaigns together with the enhanced AMVs from CIMSS and the observations from the 2015 operational HWRF (Tallapragada et al. 2015). More details and the impacts of these various observations can be found in Lu and Wang (2020).

b. *Experiment design*

To understand how the 4DIAU, 4DAN and their variants discussed in section 2 work in real cases with a highly nonlinear situation, six experiments are conducted in this study during the RI period of Hurricane Patricia (2015). The experiments are denoted as 4DEV, 4DIAU, 4DIAU-RL, 4DAN, 4DAN-RL, and 4DIAU-FR. Details of each experiment are described as below.

Experiment 4DEV is the baseline experiment, where forecasts initialized from the 4DEnVar analysis is used for reference. In this experiment, the triple nested background at 18-/6-/2-km grid spacing and the double nested ensemble forecasts at 18-/6-km grid spacing were generated from a continuously cycled HWRF DA system from Lu and Wang (2019). Both the ensemble and control backgrounds were first relocated by assimilating the TCVital positions using an EnSRF algorithm (Whitaker and Hamill 2002) prior DA to reduce the nongaussianity due to large location errors. Then 4DEnVar DA is performed to assimilate the observations listed in Table 1 between 1500 and 2100 UTC 22 October 2015. During the dual-resolution 4DEnVar DA, the background at 2 km is ingesting the 40-member ensemble error covariance at 6-km grid spacing. And the background at 6 km is ingesting the 6-km ensemble error covariance as well. More details about the relocation, 4DEnVar methodology and the DA system can be found in Lu et al. (2017b). Next, the DA analyses are downscaled to the 6-/2-/0.67-km grid spacing through interpolation. Finally, a 42-h forecast is initialized from the downscaled analysis valid at 1800 UTC 22 October 2015. This 42-h forecast is denoted as 4DEV, and the downscaled analyses will be used to calculate the predetermined increments for other 4DIAU experiments. In this current study, due to computational cost constraint, subkilometer resolution is only used during the free forecast but not during the DA. Further investigations on how the model resolution change impacts before and after DA are discussed in Feng and Wang (2021).

The traditional 4DIAU is performed in experiment 4DIAU (a schematic is shown in Fig. 3). The predetermined increments are calculated as follows. First, one 6-h background forecast named as "NoDA" is generated at the 6-/2-/0.67-km grid spacing to prepare the predetermined increments for 4DIAU. To do so, the background forecast valid at 1500 UTC 22 October 2015 from Lu and Wang (2019) is downscaled from 18/6/2 km. No relocation is performed in this background before or after downscaling. Then, the 6-h forecast is initialized from this downscaled background up to 2100 UTC 22 October. Second, the predetermined increments are calculated between the downscaled 4DEnVar analyses and the NoDA forecasts. For 4DIAU, the predetermined increments are added to each model integration time step, which is every 12 s, through the forcing term following Eq. (4).

Experiment 4DIAU-RL is similar to experiment 4DIAU except that the downscaled background forecast valid at 1500 UTC 22 October is relocated to the interpolated best track[1] before initialization. This relocated background is named as NoDA-RL to distinguish from NoDA. Such a correction in the initial location error of real storm is equivalent to the correction of initial phase error in the idealized model. By design, the NoDA-RL forecasts have much smaller location errors as compared to those in NoDA, and so are the predetermined increments as suggested in section 2b. Hence, the comparison

[1] The best track data are from the National Hurricane Center and only available at the synoptic times. The data can be found online at https://www.nhc.noaa.gov/data/hurdat/hurdat2-1851-2019-052520.txt. The relocation is achieved through the HWRF vortex relocation procedure.

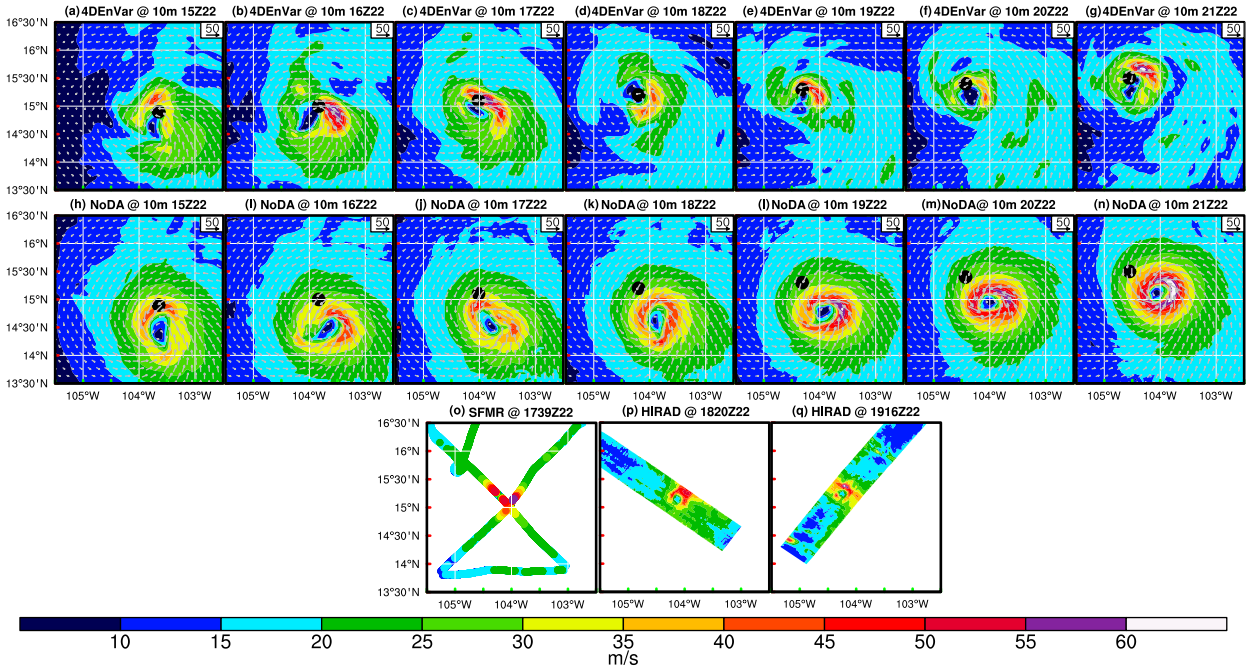

FIG. 4. The hourly evolution of the 10-m wind field for (a)–(g) the 4DEnVar analyses, and (h)–(n) the NoDA forecasts between 1500 and 2100 UTC 22 Oct 2015. (o) The SFMR observations centered at 1739 UTC and HIRAD observations centered at (p) 1820 UTC and (q) 1916 UTC 22 Oct 2015 are shown for reference. The black dot in each figure is the best track (interpolated for nonsynoptic times) at the corresponding time.

between experiments 4DIAU-RL and 4DIAU can help reveal the contribution of the initial location error during the degraded 4DIAU analysis and forecast as discussed in section 2c for the real cases.

Similar to 4DIAU and 4DIAU-RL, experiments 4DAN and 4DAN-RL are designed following section 2 and Eq. (6). No predetermined increments are calculated with the 4DAN configurations. Instead, 4DAN calculates online increments between the analyses and the model forecast initialized from NoDA at 1500 UTC 22 October 2015. To be more specific, a weighted difference between the model forecast and the 4DEnVar analyses at each time step is added to the model as an external forcing term following Eq. (6) to gradually nudge the model forecast toward 4DEnVar analyses. The 4DAN-RL experiment differs from 4DAN by initializing from NoDA-RL at the initial time. Comparisons between 4DAN (4DAN-RL) and 4DIAU (4DIAU-RL) aim to demonstrate the issue of the implicit linear assumption in using the predetermined increments during the 4DIAU methods in a real hurricane case. And the comparisons between 4DAN and 4DAN-RL shall help further identify the impact of the initial location errors for the incremental updates.

Following section 2d, experiment 4DIAU-FR does not relocate the background forecast, instead, it relocates all the downscaled 4DEnVar analyses to the positions of the storm in NoDA and then calculates the storm-relative increments to form forcing terms. This was achieved by leveraging the moving nest capability of HWRF. At the end of a 6-h IAU time window, the 4DIAU-FR forecast will be relocated back to the observed storm location and then a 39-h free forecast is initialized to the end of the storm. The comparison among 4DIAU, 4DIAU-RL, and 4DIAU-FR is to further reveal the use of classic 4DIAU for a case associated with nonlinear hurricane evolution and to demonstrate the value of the proposed 4DIAU variants: 4DIAU-RL and 4DIAU-FR.

4. Results

a. 4DEnVar, 4DIAU, and 4DAN forecasts

The wind fields of the 4DEnVar DA analyses and the corresponding NoDA forecasts at the surface are first shown in Fig. 4 verified against the SFMR and the Hurricane Imaging Radiometer (HIRAD; Cecil et al. 2017) observations. Figures 4h–4n show that the NoDA forecast is initially larger in size than the observations. Assimilating high-resolution inner-core observations as listed in section 3a using 4DEnVar produces a significantly reduced storm size and a more asymmetric primary circulation. These features in the analyses are more consistent with the observations than the background, except that the wind maximum at 1800 UTC is positioned to the southeast rather than northeast (Fig. 4d). This analysis at 1800 UTC 22 October 2015 will then be used as the initial condition for the 4DEV forecast as designed in section 3b.

The intensity and track predictions of 4DEV is shown in Fig. 5 in comparison with the best track. When initialized from the analysis at 1800 UTC, both track and intensification rate predictions of 4DEV during the intensification period of Patricia do not match the observations. Specifically, an

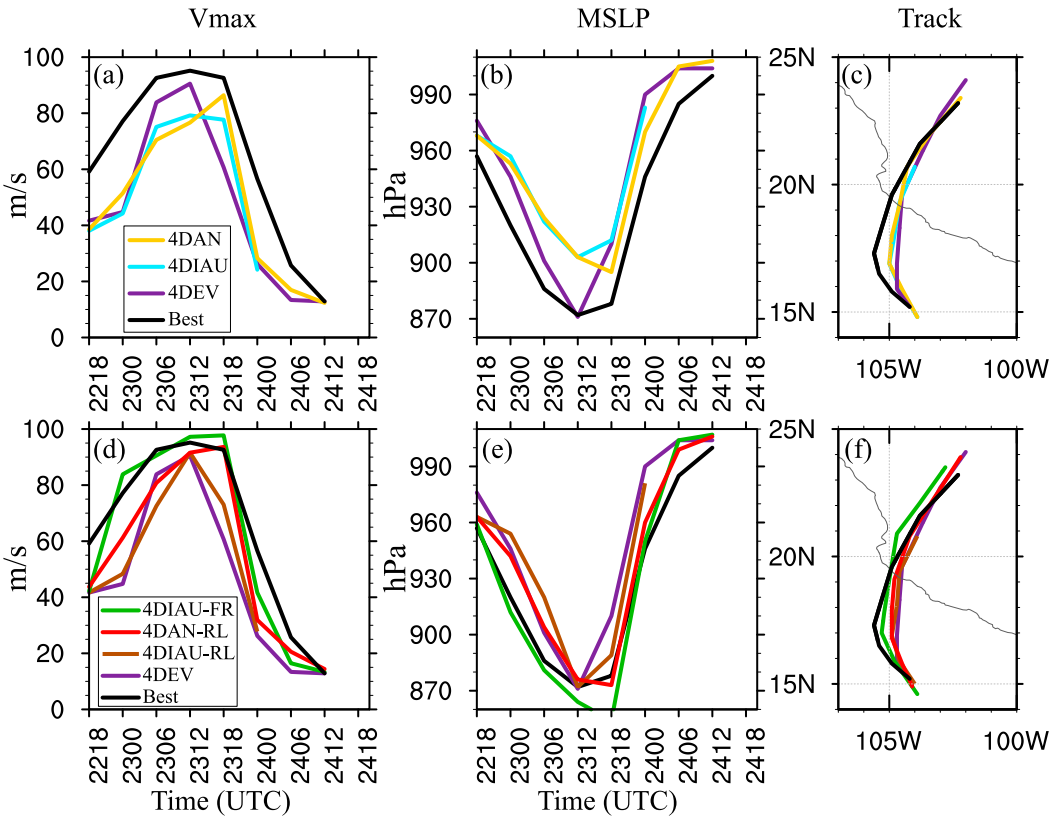

FIG. 5. The (a),(d) Vmax; (b),(e) MSLP; and (c),(f) track predictions of the experiments 4DEV (purple), 4DIAU (cyan), 4DAN (gold), 4DIAU-RL (brown), 4DAN-RL (red), and 4DIAU-FR (green) in comparison with the best track (black) during Patricia. Note, to be comparable with 4DEV and the best track, all the forecasts are plotted from 1800 UTC, even though the actual free forecast in the IAU and AN experiments started from 2100 UTC.

eastward bias is noticed in the track predictions from 4DEV (Fig. 5c). In addition, the Vmax evolution in the best track suggests that the storm was rapidly intensifying at an almost constant rate (Fig. 5a). In comparison, 4DEV shows a much slower Vmax intensification in the first 6 h and then intensifies much faster afterward. The 4DEV experiment eventually reaches a peak intensity that is about 5 m s^{-1} less than the best track at 1200 UTC 23 October. For the minimum sea level pressure (MSLP), 4DEV intensifies at a consistently faster rate than the best track during the intensification period with a weaker initial value (Fig. 5b). Such an inconsistent Vmax and MSLP evolution indicates an imbalanced wind and pressure field. As discussed earlier in section 1, the slow Vmax intensification in the first 6 h of 4DEV is likely attributed to the model shock in response to DA after a dramatically size change. To support the hypothesis, an extra experiment "Back," which is initialized from the downscaled DA background valid at 1800 UTC is performed in consistency with 4DEV to reveal the shock. The mean absolute sea level pressure (MASLP) tendency evolution for the 4DEV and the corresponding Back forecast is shown in Fig. 6. The comparison between Back and 4DEV indicates that the intermittent DA can add about 20% more shocks to the model in this case. To better understand the impact of these shocks or instabilities to 4DEV, a time–radius Hovmöller diagram of the eyewall evolution is given in Fig. 7a. While the azimuthal mean tangential field indicates a gradually reducing storm size in 4DEV, its azimuthal mean vertical velocity evolution is struggling to establish a well-defined eyewall. Multiple updraft maxima continuously pop up even inside the eye region of 4DEV, which suggests dramatic dynamical adjustments even after hours of model integration.

The 4DIAU experiment is supposed to reduce such a shock and improve the short-term intensity prediction by design. As detailed in section 3b (Figs. 4h–n), the predetermined increments are calculated based on the NoDA forecasts and the downscaled 4DEnVar analyses, and are added incrementally to 4DIAU. Consistent with our expectation, Fig. 6 indicates that using the incremental update in 4DIAU introduces almost no additional shock to the model as compared to NoDA. The eyewall evolution in Fig. 7b also indicates less dynamical imbalance as the spurious updrafts in the eye region are not found in 4DIAU in contrast to 4DEV. The surface wind evolution of 4DIAU during the 6-h IAU time window is shown in Figs. 8a–8g. The 4DIAU experiment gradually reduces its storm size, increases its asymmetry, and reduces the location error as the increments are incrementally added to the model integration. However, an apparent issue is noticed in the 4DIAU forecasts. The intensity of this updated storm is even weaker than the

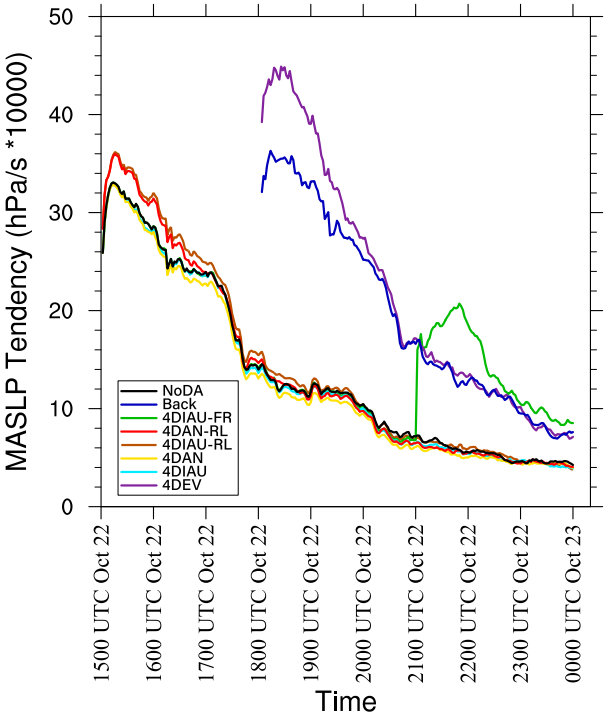

FIG. 6. The mean absolute sea level pressure (MASLP) tendency evolution of the NoDA (black), Back (blue), 4DEV (purple), 4DIAU (cyan), 4DAN (gold), 4DIAU-RL (brown), 4DAN-RL (red), and 4DIAU-FR (green) between 1500 UTC 22 Oct and 0000 UTC 23 Oct. The tendency is output every 2 min.

background (e.g., Fig. 8d vs Fig. 4r). With this even weaker Vmax during the update, the 4DIAU reaches a weaker peak Vmax as compared to 4DEV around 1200 UTC 23 October (Fig. 5a). Although the MSLP seems to be enhanced by the 4DIAU during the incremental updates, it strengthens more slowly afterward in consistency with the Vmax evolution (Fig. 5b). The eastward bias is only slightly reduced in the track forecast as shown in Fig. 5c.

In general, the storm evolution in 4DIAU is not improved upon 4DEV although the model shock is reduced. Consistent with section 2b, it is hypothesized that using predetermined increments in 4DIAU can bring disruptive effect while the storm went through rapidly changing nonlinear evolution. The predetermined increments used for 4DIAU at each analysis time are shown in Figs. 8h–8n. Specifically, these increments are subtracted from the 4DEnVar analyses in Figs. 4h–4n using the NoDA forecasts in Figs. 4o–4u. Given both large location and size corrections, the decrease of wind speed dominates the predetermined increments most of the time, except around the wind maxima of the analysis and the eye regions of the background. These predetermined increments tend to build a cyclonic circulation near the analyzed storm and an anticyclonic circulation near the background storm. As shown in section 2b, when the modified storm shifts away from the background forecast due to nonlinear evolution, these predetermined increments can be added to wrong locations and therefore cause issues in IAU analysis and prediction. To better visualize such an impact, the predetermined increments (Figs. 8h–n) are directly added to the corresponding 4DIAU forecasts (Figs. 8a–g) to produce combined ''analyses'' in Figs. 8o–8u. Initially at 1500 UTC when there is no increment added to the model yet, the combined analysis is exactly the same as the 4DEnVar analysis. And there are not many differences between these two analyses for the first several hours when the IAU influenced storm barely diverges from the NoDA forecast (Figs. 8p–q). As the updated forecast from 4DIAU gradually deviates away from NoDA at the later hours (Figs. 8r–u), the structures of the combined analyses significantly differ from the 4DEnVar analyses because the predetermined increments calculated from NoDA are now inconsistently added to the 4DIAU influenced forecast. Specifically, instead of modifying the storm size and location, the predetermined increments now tend to create a strong and localized jet (Figs. 8t–u), which is destructive to the storm structure. As a result, the model struggles to maintain a reasonable storm structure during the IAU period. As evidenced in Fig. 7b, the eyewall region becomes too wide and has multiple maxima between 1700 and 2000 UTC. Between 2100 and 2300 UTC, there is even an eyewall replacement feature in the 4DIAU forecast, which should not happen during the RI period of Patricia but 24 h later in reality (Rogers et al. 2017).

In agreement with the hypotheses and discussions in section 2b, results in this subsection indicate that the major issue of 4DIAU is from the use of predetermined increments while the hurricane goes through rapidly changing nonlinear evolution. The 4DAN experiment is expected to suffer less on this issue. Figure 9a–9g shows that 4DAN not only successfully reduces the storm size, increases the storm asymmetry, and reduces the storm location error gradually as 4DIAU, but also improves the intensity predictions upon 4DIAU, especially at the early lead times (Figs. 5a,b). However, as shown in Figs. 9g and 5, the Vmax evolution of 4DAN is still too weak to begin with, and its peak is about 9 m s^{-1} weaker than the best track (Fig. 5a). Moreover, the MSLP evolution of 4DAN after 0000 UTC 23 October is also much weaker than the best track (Fig. 5b). Figure 7c indicates that although the eyewall evolution in 4DAN has better continuity than 4DIAU, its eyewall is still wide and is not very well-organized as an RI storm. Figure 6 shows that 4DAN produces the least MASLP tendency among all the experiments, which is even weaker than NoDA at almost all times. Such a result is likely related to the overly strong filtering effect of nudging on the background field as discussed in sections 1 and 2b.

b. *4DIAU-RL and 4DAN-RL forecasts*

In section 4a, although both 4DIAU and 4DAN experiments show less shocks to the model as expected, they under forecast the intensity compared to 4DEV As suggested in section 2c, removing the initial location error should improve both methods. Thus, experiments 4DIAU-RL and 4DAN-RL as designed in section 3b are conducted.

The 4DIAU-RL forecast is shown in Figs. 10a–10g. To begin with, the background valid at 1500 UTC is first relocated to the best track (NoDA-RL). The extra relocation step in the background introduces additional shocks to the model as shown in

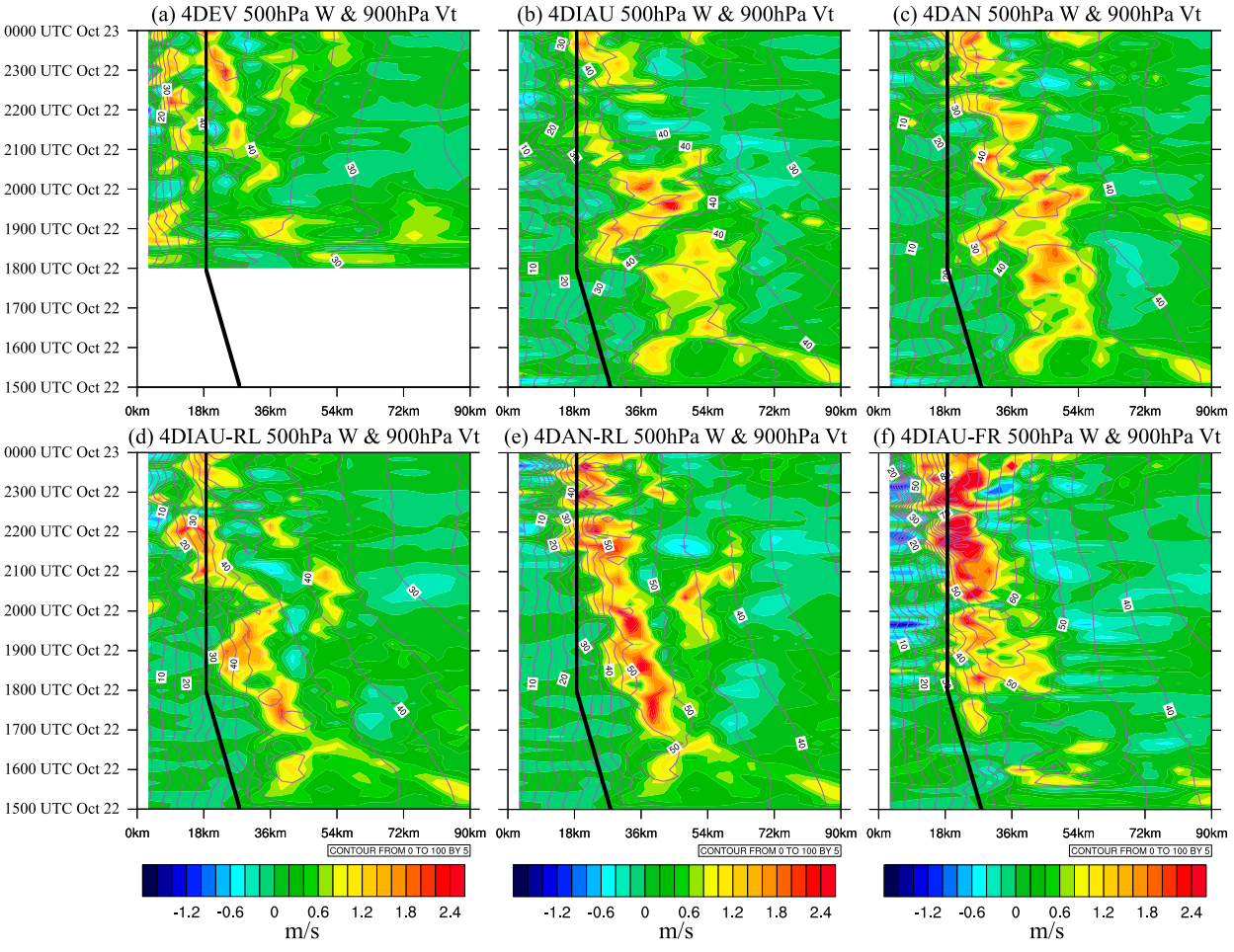

FIG. 7. The time–radius Hovmöller diagram of the azimuthal mean vertical velocity at 500 hPa (shaded) and the azimuthal mean tangential wind at 900 hPa (gray contour) for (a) 4DEV, (b) 4DIAU, (c) 4DAN, (d) 4DIAU-RL, (e) 4DAN-RL, and (f) 4DIAU-FR between 1500 UTC 22 Oct and 0000 UTC 23 Oct. The corresponding radius of maximum wind evolution from the postseason b-deck best track is shown in black.

Fig. 6 (brown vs cyan). But this increase of MASLP tendency is apparently smaller than the increase due to the intermittent DA in 4DEV (purple vs blue). With a much smaller location error at the initial time[2] (Fig. 10a vs Fig. 8a), the location errors within the 6-h time-window are smaller and are reflected as reduced dipole features and smaller magnitude of the predetermined increments (Figs. 10h–n). The smaller predetermined increments lead to smaller discrepancy of 4DIAU-RL between the updated and background forecasts. Consequently, the combined analyses from 4DIAU-RL (Figs. 10o–u) suggest a more reasonable storm evolution as compared to that in 4DIAU. For example, the jet like feature of the combined analysis for 4DIAU-RL is much less significant than that in 4DIAU (Fig. 10u vs Fig. 8u). Therefore 4DIAU-RL eventually produces a stronger forecast (Figs. 5d–e) with more size corrections as compared to 4DIAU (Fig. 10g vs Fig. 8g). The vertical velocity evolution in 4DIAU-RL also shows a more reasonable and consistent eyewall contraction evolution during and after the IAU period than 4DIAU (Fig. 7c vs Fig. 7b). Such an improvement of 4DIAU-RL over 4DIAU is in agreement with our results in section 2b. However, as indicated in section 2b, since there is still a moving speed discrepancy between the updated and background forecast, the less initial location error in 4DIAU-RL can only alleviate the nonlinear issues to certain extent. Hence, although the intensification rate of Vmax predictions is improved upon 4DIAU, 4DIAU-RL only improves the Vmax and MSLP predictions upon 4DEV for the first several hours. The intensification rate in 4DIAU-RL is still too weak as compared to the best track and the peak intensity around 1200 UTC 23 October is only slightly better than 4DEV (Figs. 5d,e). Furthermore, despite the smaller initial track error, the track prediction in 4DIAU-RL is overall comparable with 4DIAU (Fig. 5c vs Fig. 5e).

Similar to 4DIAU-RL, 4DAN-RL is also initialized from NoDA-RL with less initial location error as compared to 4DAN. Figures 9h–9n show that this 4DAN-RL clearly

[2] The relocation is not able to fully remove the location error because the accuracy of the relocation package is on the order of 0.1°.

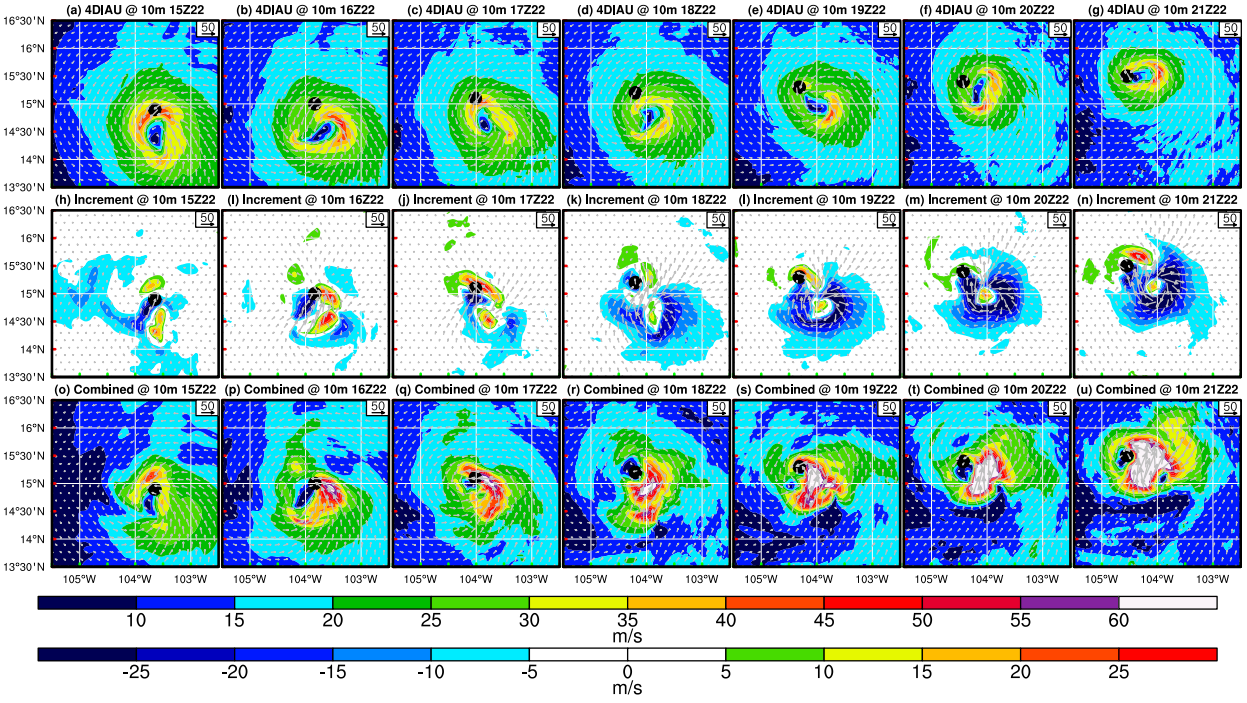

FIG. 8. As in Fig. 4, but for (a)–(g) 4DIAU forecasts, (h)–(n) the predetermined increments, and (o)–(u) the combined analyses.

produces stronger Vmax evolution than 4DAN in addition to the size correction during the updates. Additionally, the Vmax and MSLP predictions in Figs. 5d and 5e show that 4DAN-RL not only improves the intensity prediction over 4DAN, but also improves the intensity prediction over the corresponding 4DIAU-RL as well as 4DEV at almost all lead times. The vertical velocity evolution in Fig. 7e shows that 4DAN-RL produces a consistently intensifying and contracting eyewall, which agrees with the intensifying Patricia better than 4DAN. Also, 4DAN-RL again produces a smoother and more continuous eyewall evolution than 4DIAU-RL, especially near the end of the IAU period at 2100 UTC 22 October. It is noticed that the eyewall of 4DAN-RL between 2100 UTC 22 October and 0000 UTC 23 October is slightly stronger than that in 4DIAU-RL (Fig. 7e vs Fig. 7d). These results are consistent with the stronger intensity predictions from 4DAN-RL in Fig. 5. The MASLP tendency evolution in Fig. 6 suggests that nudging is again producing slightly less shocks to the model as compared to the corresponding 4DIAU-RL. The track forecast from 4DAN-RL is not significantly better than either 4DAN or 4DIAU-RL.

c. *4DIAU-FR forecasts*

To further improve the application of 4DIAU in the rapidly evolving hurricane predictions, a 4DIAU-FR approach is

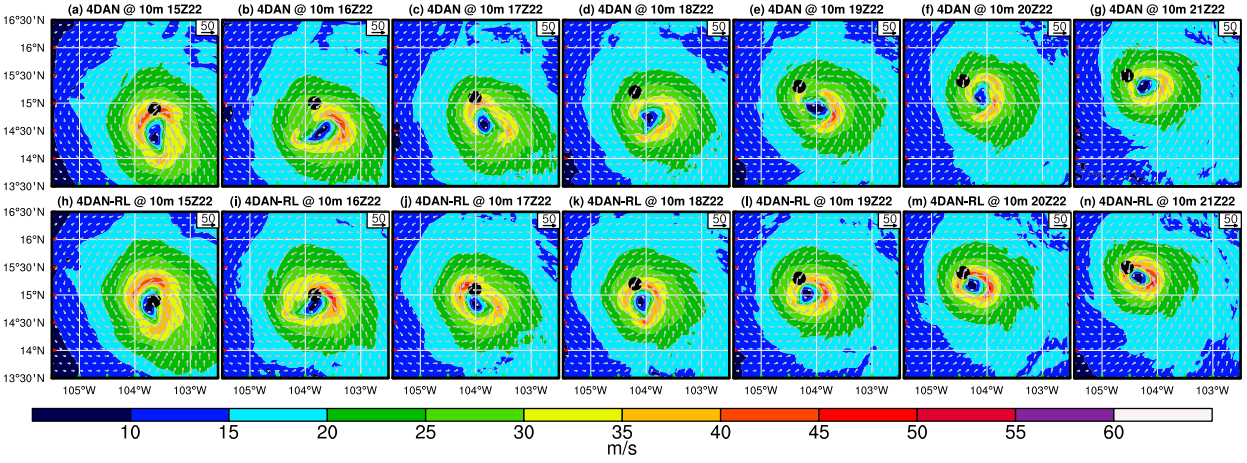

FIG. 9. As in Fig. 4, but for (a)–(g) 4DAN forecasts and (h)–(n) 4DAN-RL forecasts.

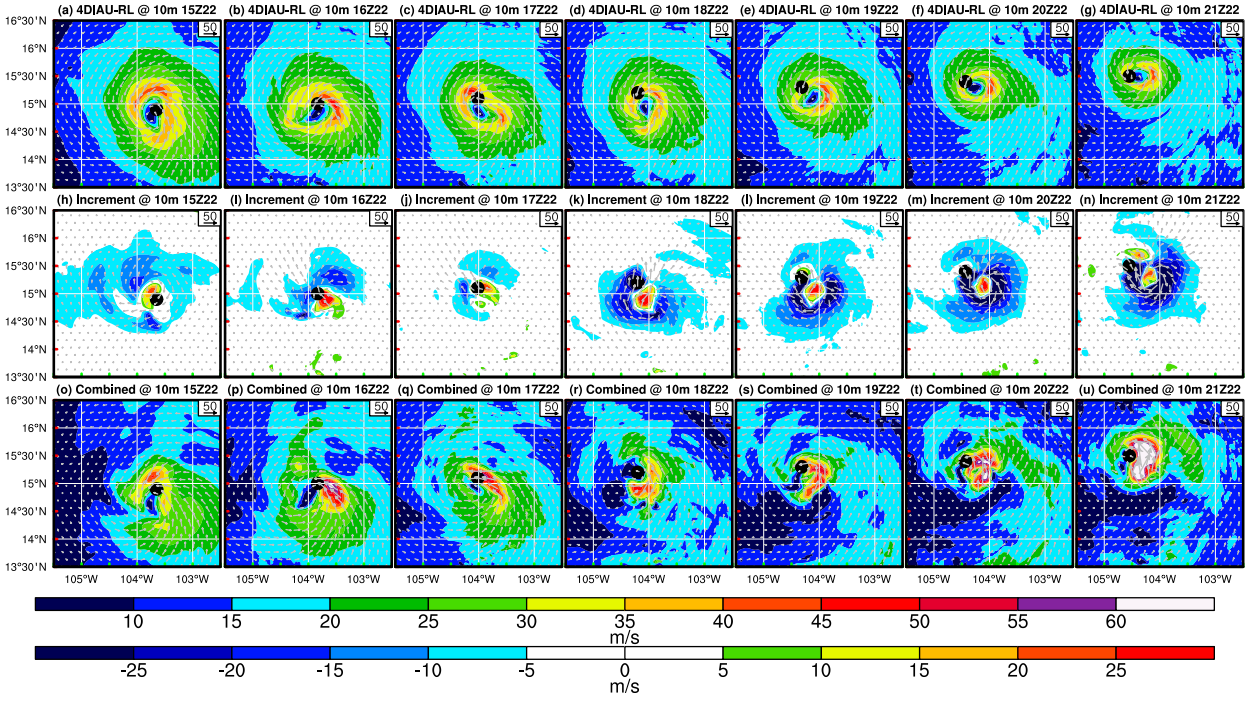

FIG. 10. As in Fig. 8, but for 4DIAU-RL.

proposed in section 2d. This approach calculates feature (storm in this case) relative increment and is not concerned by the moving speed discrepancy between the updated and background forecasts. The 4DIAU-FR forecast is shown in Figs. 11a–11g. The analyzed TC from 4DIAU-FR is significantly stronger than either 4DIAU or 4DIAU-RL while the storm size is consistently reduced during the incremental updates (Figs. 11a–g). Note that the final 4DIAU-FR analysis on 2100 UTC 22 October in Fig. 11g is relocated to the observed position before initializing the prediction (Fig. 11h). Such a relocation can introduce

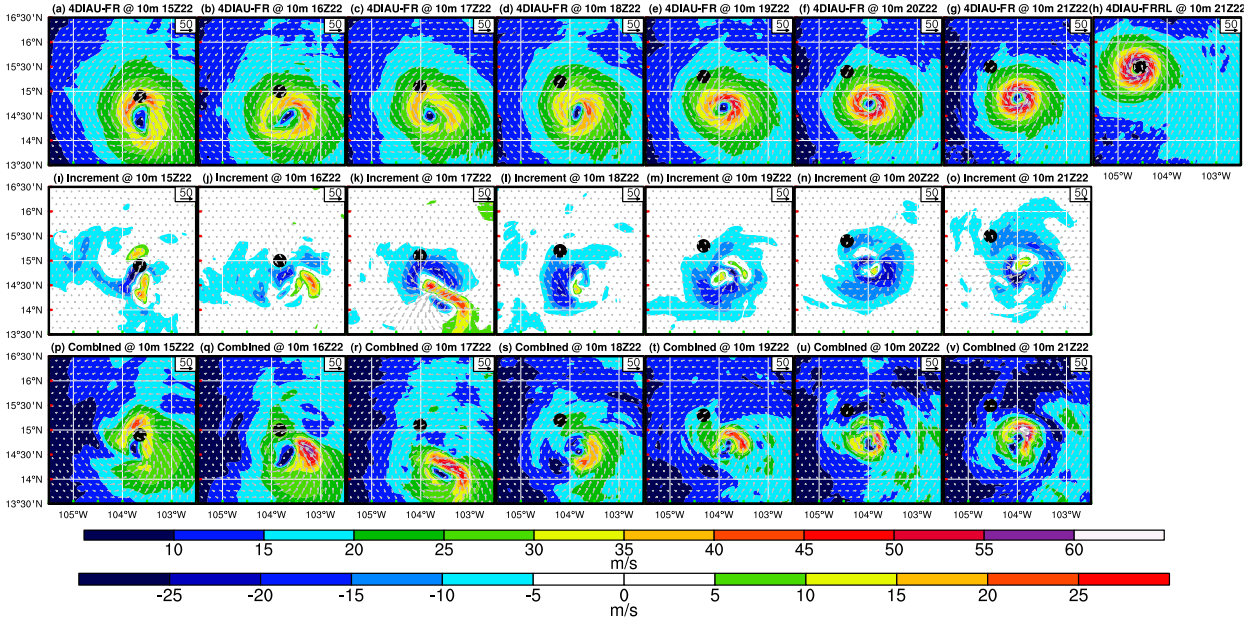

FIG. 11. (a)–(v) As in Fig. 8, but for 4DIAU-FR. The 4DIAU-FR forecast at the final IAU times at 2100 UTC 22 Oct 2015 will be relocated to the best track and is shown in (h).

additional shocks to the model, but the shocks are not as significant as those from the downscaling at 1500 UTC (Fig. 6, green vs cyan). Despite the shock to the model at the end of the incremental update, the eyewall evolution in Fig. 7f suggests that 4DIAU-FR is hardly degraded by the shocks. In fact, the updraft in 4DIAU-FR is consistently stronger than any other experiments beginning from the end of the IAU period at 2100 UTC, consistent with the stronger intensity predictions from Figs. 5d–5f. The predicted MSLP and Vmax values from 4DIAU-FR match the best track the most among all experiments during the intensification period, except that the peak values are too strong, especially the MSLP. The overly low MSLP is likely due to a systematic bias from the HWRF Model as we found in Lu and Wang (2021), which the HWRF tends to over predict MSLP when Vmax matches the best track for strong storms. The track prediction from 4DIAU-FR also matches the best track better than any other experiments. These significant improvements upon all the other experiments in 4DIAU-FR are consistent with our conclusions from the idealized experiments in section 2d.

The improvements of 4DIAU-FR over both 4DIAU and 4DIAU-RL again suggest that the moving speed discrepancy during the nonlinear evolution is one major problem of the predetermined increments used by the 4DIAU methods for hurricane predictions. The predetermined feature-relative increments in 4DIAU-FR show reduction of wind speed primarily outside the radius of maximum wind (RMW) and increase of wind speed inside, which corresponds to primarily the size reduction of the storm (Figs. 11i–o). The combined analyses in Figs. 11p–11v show reasonable storms with reduced sizes at all lead times. Unlike 4DIAU, the RI of the 4DIAU-FR storm during the size contraction is not interrupted by the false corrections due to the moving speed discrepancy. These results suggest that the 4DIAU-FR method is potentially an efficient approach to improve the application of 4DIAU for the rapidly evolving hurricane predictions.

5. Summary and discussion

This study explores the limitation and potential improvements of the 4DIAU methods for the short-term intensity prediction of hurricanes using a GSI-based 4DEnVar DA system for HWRF.

The degradation of the traditional 4DIAU in highly nonlinear evolutions is first identified and investigated using a simple oscillation model. Using the online increments with a 4DAN method is found to reduce the degradation but increases amplitude errors. Further investigations show that reducing initial phase error can help reduce the degradation in 4DIAU as well as in 4DAN. To fully address the degradation issue in the 4DIAU method, one feature-relative method is proposed and is found to significantly improve the forecasts under nonlinear evolutions as compared to the other experiments.

The 4DIAU, 4DAN, and the proposed improvements are then implemented into the GSI-based 4DEnVar DA system for HWRF. Experiments are conducted with real case storm Patricia (2015) based on an early study by Lu and Wang (2019). The overall results in the intensity predictions of Patricia are in line with the findings from the simple oscillation model. Specifically, 4DEV improves the storm structure by reducing the storm size and increasing the storm asymmetry but is suffering from slow spinup due to dramatic dynamical adjustments in the model after initialization. The 4DIAU experiment gradually modifies the storm structure by reducing its size with less shock to the model, improves the early lead-time intensity predictions by increasing the intensification rate, and slightly improves the track predictions. However, the storm produced by 4DIAU is too weak. The 4DAN experiment can improve the intensity prediction upon 4DIAU, but its peak intensity is still weaker than both the best track and 4DEV. Both 4DIAU-RL and 4DAN-RL improve the intensity prediction upon the corresponding 4DIAU and 4DAN by relocating the initial background before the incremental update. The 4DAN-RL experiment can further improve the intensity prediction upon 4DIAU-RL. The feature-relative experiment 4DIAU-FR shows the most improvement among all experiments during the incremental update and also produces the best intensity and track prediction.

In general, results from both the simple model and HWRF Model demonstrate the hypothesis that the predetermined increments used in the traditional 4DIAU are not directly applicable for the highly nonlinear systems like the rapidly intensifying hurricanes. The implicit linear violation is primarily due to the moving speed discrepancy between the updated and background forecasts during the incremental update in a nonlinear evolution. The predetermined increments in 4DIAU can be added to wrong places and damage the updating storm when such a discrepancy exists. The online or adaptive increments in 4DAN do not require the implicit linear assumption and therefore improves the performance of the incremental updates as well as the intensity prediction upon 4DIAU. But the improvements from 4DAN can be limited by its overfiltering effect.

In both 4DAN-RL and 4DIAU-RL methods, relocating the initial background during the update improves the corresponding traditional methods. Such an improvement is likely due to that the relocation not only reduces the overall location error during the updates, but also decreases the magnitude of the total increments to be addressed. Yet both the 4DIAU-RL and 4DAN-RL could double the computing cost of the incremental approach for real time use because they both require a background rerun after relocation (the initial background forecast is still needed for the 4DEnVar DA), and before the incremental update.

On the other hand, 4DIAU-FR does not require an additional background rerun in a continuously cycled DA system and it bypasses the moving speed discrepancy issue through a feature-relative framework. This approach is shown to produce the best intensity and track predictions among all experiments. However, the impact of this 4DIAU-FR is highly relied on the relocation of analyses. Our sensitivity experiments indicate that the analysis relocation tends to decrease the strength of the analysis due to the smoothing during relocation, especially when the storm is weak (not shown). Such a loss of strength in the relocated analyses can result in a loss of increments and

eventually makes the 4DIAU-FR forecast weaker than it should be (not shown).

As an initial study with limited computational resources, the methods proposed are demonstrated with a simple model and a single hurricane case. A larger sample size with a continuously cycled experiment configurations to establish a more robust conclusion about which method is the most efficient way for improving the intensity predictions of hurricanes are left for future work. Additional applications of this newly proposed 4DIAU-FR approach to other featured severe weather events as well as the potential impact of 4DIAU-FR on the storm asymmetric features are also interesting topics for the future work.

Acknowledgments. The research documented in this paper is supported by Grant NA16NWS4680028. The experiments were performed on the NOAA Supercomputer Jet and OU Supercomputer Schooner. Some results and descriptions were included in the abstract of the authors' AMS conference presentation and progress reports to the funding agencies.

Data availability statement. All the observational data and global analysis used for the HWRF Models, and the model data produced during this study, have been archived locally and are available upon request to the corresponding author.

REFERENCES

Aksoy, A., S. D. Aberson, T. Vukicevic, K. J. Sellwood, S. Lorsolo, and X. J. Zhang, 2013: Assimilation of high-resolution tropical cyclone observations with an ensemble Kalman filter using NOAA/AOML/HRD's HEDAS: Evaluation of the 2008–11 vortex-scale analyses. *Mon. Wea. Rev.*, **141**, 1842–1865, https://doi.org/10.1175/MWR-D-12-00194.1.

Bao, J.-W., and R. M. Errico, 1997: An adjoint examination of a nudging method for data assimilation. *Mon. Wea. Rev.*, **125**, 1355–1373, https://doi.org/10.1175/1520-0493(1997)125<1355:AAEOAN>2.0.CO;2.

Benkiran, M., and E. Greiner, 2008: Impact of the incremental analysis updates on a real-time system of the North Atlantic Ocean. *J. Atmos. Oceanic Technol.*, **25**, 2055–2073, https://doi.org/10.1175/2008JTECHO537.1.

Bernardet, L., V. Tallapragada, C. Holt, S. Trahan, M. Biswas, L. Carson, H. Shao, and C. Zhou, 2015: Transition of research to the operational hurricane WRF model: The role of the Developmental Testbed Center. *Sixth NOAA Testbeds and Proving Grounds Workshop*, Boulder, CO, NOAA, http://www.testbeds.noaa.gov/events/2015/workshop/presentations/wed-bernardet-hwrf.pdf.

Bloom, S. C., L. L. Takacs, M. da Silva, and D. Ledvina, 1996: Data assimilation using incremental analysis updates. *Mon. Wea. Rev.*, **124**, 1256–1271, https://doi.org/10.1175/1520-0493(1996)124<1256:DAUIAU>2.0.CO;2.

Buehner, M., and Coauthors, 2015: Implementation of deterministic weather forecasting systems based on ensemble–variational data assimilation at Environment Canada. Part I: The global system. *Mon. Wea. Rev.*, **143**, 2532–2559, https://doi.org/10.1175/MWR-D-14-00354.1.

Cecil, D. J., and S. K. Biswas, 2017: Hurricane Imaging Radiometer (HIRAD) wind speed retrievals and validation using dropsondes. *J. Atmos. Oceanic Technol.*, **34**, 1837–1851, https://doi.org/10.1175/JTECH-D-17-0031.1.

Daley, R., 1978: Variational non-linear normal mode initialization. *Tellus*, **30**, 201–218, https://doi.org/10.3402/tellusa.v30i3.10335.

Doyle, J. D., and Coauthors, 2017: A view of tropical cyclones from above: The Tropical Cyclone Intensity (TCI) experiment. *Bull. Amer. Meteor. Soc.*, **98**, 2113–2134, https://doi.org/10.1175/BAMS-D-16-0055.1.

Ek, M. B., K. E. Mitchell, Y. Lin, E. Rogers, P. Grunmann, V. Koren, G. Gayno, and J. D. Tarpley, 2003: Implementation of Noah land surface model advances in the National Centers for Environmental Prediction operational mesoscale Eta model. *J. Geophys. Res.*, **108**, 8851, https://doi.org/10.1029/2002JD003296.

Feng, J., and X. Wang, 2021: Impact of increasing horizontal and vertical resolution during the HWRF Hybrid EnVar data assimilation on the analysis and prediction of Hurricane Patricia (2015). *Mon. Wea. Rev.*, **149**, 419–441, https://doi.org/10.1175/MWR-D-20-0144.1.

Grell, G. A., 1993: Prognostic evaluation of assumptions used by cumulus parameterizations. *Mon. Wea. Rev.*, **121**, 764–787, https://doi.org/10.1175/1520-0493(1993)121<0764:PEOAUB>2.0.CO;2.

Han, J., and H. Pan, 2011: Revision of convection and vertical diffusion schemes in the NCEP Global Forecast System. *Wea. Forecasting*, **26**, 520–533, https://doi.org/10.1175/WAF-D-10-05038.1.

——, M. L. Witek, J. Teixeira, R. Sun, H. L. Pan, J. K. Fletcher, and C. S. Bretherton, 2016: Implementation in the NCEP GFS of a hybrid Eddy-Diffusivity Mass-Flux (EDMF) boundary layer parameterization with dissipative heating and modified stable boundary layer mixing. *Wea. Forecasting*, **31**, 341–352, https://doi.org/10.1175/WAF-D-15-0053.1.

Harms, D. E., S. Raman, and R. Madala, 1992: An examination of four-dimensional data-assimilation techniques for numerical weather prediction. *Bull. Amer. Meteor. Soc.*, **73**, 425–440, https://doi.org/10.1175/1520-0477(1992)073<0425:AEOFDD>2.0.CO;2.

Heng, B. C. P., and Coauthors, 2020: SINGV-DA: A data assimilation system for convective-scale numerical weather prediction over Singapore. *Quart. J. Roy. Meteor. Soc.*, **146**, 1923–1938, https://doi.org/10.1002/qj.3774.

Hoke, J. E., and R. A. Anthes, 1976: The initialization of numerical models by a dynamic-initialization technique. *Mon. Wea. Rev.*, **104**, 1551–1556, https://doi.org/10.1175/1520-0493(1976)104<1551:TIONMB>2.0.CO;2.

Hong, S.-Y., and H.-L. Pan, 1996: Nonlocal boundary layer vertical diffusion in a medium-range forecast model. *Mon. Wea. Rev.*, **124**, 2322–2339, https://doi.org/10.1175/1520-0493(1996)124<2322:NBLVDI>2.0.CO;2.

Huang, X.-Y., and P. Lynch, 1993: Diabatic digital-filtering initialization: Application to the HIRLAM model. *Mon. Wea. Rev.*, **121**, 589–603, https://doi.org/10.1175/1520-0493(1993)121<0589:DDFIAT>2.0.CO;2.

Iacono, M. J., J. S. Delamere, E. J. Mlawer, M. W. Shephard, S. A. Clough, and W. D. Collins, 2008: Radiative forcing by long-lived greenhouse gases: Calculations with the AER radiative transfer models. *J. Geophys. Res.*, **113**, D13103, https://doi.org/10.1029/2008JD009944.

Kaplan, J., M. DeMaria, and J. A. Knaff, 2010: A revised tropical cyclone rapid intensification index for the Atlantic and eastern North Pacific basins. *Wea. Forecasting*, **25**, 220–241, https://doi.org/10.1175/2009WAF2222280.1.

Lee, M.-S., Y.-H. Kuo, and D. M. Barker, 2006: Incremental analysis updates initialization technique applied to 10-km

MM5 and MM5 3DVAR. *Mon. Wea. Rev.*, **134**, 1389–1404, https://doi.org/10.1175/MWR3129.1.

Lei, L., and J. S. Whitaker, 2016: A four-dimensional incremental analysis update for the ensemble Kalman filter. *Mon. Wea. Rev.*, **144**, 2605–2621, https://doi.org/10.1175/MWR-D-15-0246.1.

Li, Y., X. Wang, and M. Xue, 2012: Assimilation of radar radial velocity data with the WRF hybrid ensemble-3DVAR system for the prediction of Hurricane Ike (2008). *Mon. Wea. Rev.*, **140**, 3507–3524, https://doi.org/10.1175/MWR-D-12-00043.1.

Lorenc, A. C., N. E. Bowler, A. M. Clayton, S. R. Pring, and D. Fairbairn, 2015: Comparison of hybrid-4DEnVar and hybrid-4DVar data assimilation methods for global NWP. *Mon. Wea. Rev.*, **143**, 212–229, https://doi.org/10.1175/MWR-D-14-00195.1.

Lu, X., and X. Wang, 2019: Improving hurricane analyses and predictions with TCI, IFEX field campaign observations, and CIMSS AMVs using the advanced hybrid data assimilation system for HWRF. Part I: What is missing to capture the rapid intensification of Hurricane Patricia (2015). *Mon. Wea. Rev.*, **147**, 1351–1373, https://doi.org/10.1175/MWR-D-18-0202.1.

——, and ——, 2020: Improving hurricane analyses and predictions with TCI, IFEX field campaign observations, and CIMSS AMVs using the advanced hybrid data assimilation system for HWRF. Part II: Observation impacts on the analysis and prediction of Patricia (2015). *Mon. Wea. Rev.*, **148**, 1407–1430, https://doi.org/10.1175/MWR-D-19-0075.1.

——, and ——, 2021: The assimilation of coastal ground-based WSR-88D and airborne tail Doppler radar observations with the hybrid 3DEnVar system to improve HWRF landfalling hurricane prediction. *34th Conf. on Hurricanes and Tropical Meteorology*, Amer. Meteor. Soc., 3C.6, https://ams.confex.com/ams/34HURR/meetingapp.cgi/Paper/373750.

——, ——, Y. Li, M. Tong, and X. Ma, 2017a: GSI-based ensemble-variational hybrid data assimilation for HWRF for hurricane initialization and prediction: Impact of various error covariances for airborne radar observation assimilation. *Quart. J. Roy. Meteor. Soc.*, **143**, 223–239, https://doi.org/10.1002/qj.2914.

——, ——, M. Tong, and V. Tallapragada, 2017b: GSI-based, continuously cycled, dual-resolution hybrid ensemble-variational data assimilation system for HWRF: System description and experiments with Edouard (2014). *Mon. Wea. Rev.*, **145**, 4877–4898, https://doi.org/10.1175/MWR-D-17-0068.1.

Lynch, P., and X. Huang, 1992: Initialization of the HIRLAM model using a digital filter. *Mon. Wea. Rev.*, **120**, 1019–1034, https://doi.org/10.1175/1520-0493(1992)120<1019:IOTHMU>2.0.CO;2.

Machenhauer, B., 1977: On the dynamics of gravity oscillations in a shallow water model, with application to normal mode initialization. *Beitr. Phys. Atmos.*, **50**, 253–271.

Macpherson, B., 2001: Operational experience with assimilation of rainfall data in the Met Office Mesoscale model. *Meteor. Atmos. Phys.*, **76**, 3–8, https://doi.org/10.1007/s007030170035.

Morel, P., and O. Talagrand, 1974: Dynamic approach to meteorological data assimilation. *Tellus*, **26**, 334–344, https://doi.org/10.3402/tellusa.v26i3.9839.

Pu, Z., S. Zhang, M. Tong, and V. Tallapragada, 2016: Influence of the self-consistent regional ensemble background error covariance on hurricane inner-core data assimilation with the GSI-based hybrid system for HWRF. *J. Atmos. Sci.*, **73**, 4911–4925, https://doi.org/10.1175/JAS-D-16-0017.1.

Qin, N., and D.-L. Zhang, 2018: On the extraordinary intensification of Hurricane Patricia (2015). Part I: Numerical experiments. *Wea. Forecasting*, **33**, 1205–1224, https://doi.org/10.1175/WAF-D-18-0045.1.

Rogers, R., and Coauthors, 2006: The Intensity Forecasting Experiment: A NOAA multiyear field program for improving tropical cyclone intensity forecasts. *Bull. Amer. Meteor. Soc.*, **87**, 1523–1538, https://doi.org/10.1175/BAMS-87-11-1523.

——, and Coauthors, 2013: NOAA's Hurricane Intensity Forecasting Experiment (IFEX): A progress report. *Bull. Amer. Meteor. Soc.*, **94**, 859–882, https://doi.org/10.1175/BAMS-D-12-00089.1.

——, and Coauthors, 2017: Rewriting the tropical record books: The extraordinary intensification of Hurricane Patricia (2015). *Bull. Amer. Meteor. Soc.*, **98**, 2091–2112, https://doi.org/10.1175/BAMS-D-16-0039.1.

Tallapragada, V., and Coauthors, 2015: Hurricane Weather Research and Forecasting (HWRF) model: 2015 scientific documentation. Developmental Testbed Center, 81 pp., http://www.dtcenter.org/HurrWRF/users/docs/scientific_documents/HWRFScientificDocumentation_August2011.pdf.

Tong, M., and Coauthors, 2018: Impact of assimilating aircraft reconnaissance observations on tropical cyclone initialization and prediction using operational HWRF and GSI ensemble-variational hybrid data assimilation. *Mon. Wea. Rev.*, **146**, 4155–4177, https://doi.org/10.1175/MWR-D-17-0380.1.

Torn, R. D., and G. J. Hakim, 2009: Ensemble data assimilation applied to RAINEX observations of Hurricane Katrina (2005). *Mon. Wea. Rev.*, **137**, 2817–2829, https://doi.org/10.1175/2009MWR2656.1.

Velden, C., W. E. Lewis, W. Bresky, D. Stettner, J. Daniels, and S. Wanzong, 2017: Assimilation of high-resolution satellite-derived atmospheric motion vectors: Impact on HWRF forecasts of tropical cyclone track and intensity. *Mon. Wea. Rev.*, **145**, 1107–1125, https://doi.org/10.1175/MWR-D-16-0229.1.

Weng, Y., and F. Zhang, 2012: Assimilating airborne Doppler radar observations with an ensemble Kalman filter for convection-permitting hurricane initialization and prediction: Katrina (2005). *Mon. Wea. Rev.*, **140**, 841–859, https://doi.org/10.1175/2011MWR3602.1.

Whitaker, J. S., and T. M. Hamill, 2002: Ensemble data assimilation without perturbed observations. *Mon. Wea. Rev.*, **130**, 1913–1924, https://doi.org/10.1175/1520-0493(2002)130<1913:EDAWPO>2.0.CO;2.

Wu, T.-C., C. S. Velden, S. J. Majumdar, H. Liu, and J. L. Anderson, 2015: Understanding the influence of assimilating subsets of enhanced atmospheric motion vectors on numerical analyses and forecasts of tropical cyclone track and intensity with an ensemble Kalman filter. *Mon. Wea. Rev.*, **143**, 2506–2531, https://doi.org/10.1175/MWR-D-14-00220.1.

Xiao, Q., X. Zhang, C. Davis, J. Tuttle, G. Holland, and P. J. Fitzpatrick, 2009: Experiments of hurricane initialization with airborne Doppler radar data for the Advanced Research hurricane WRF (AHW) Model. *Mon. Wea. Rev.*, **137**, 2758–2777, https://doi.org/10.1175/2009MWR2828.1.

Zhang, F., Y. Weng, J. Sippel, Z. Meng, and C. H. Bishop, 2009: Cloud-resolving hurricane initialization and prediction through assimilation of Doppler radar observations with an ensemble Kalman filter. *Mon. Wea. Rev.*, **137**, 2105–2125, https://doi.org/10.1175/2009MWR2645.1.

——, ——, J. F. Gamache, and F. D. Marks, 2011: Performance of convection-permitting hurricane initialization and prediction during 2008-2010 with ensemble data assimilation of inner-core airborne Doppler radar observations. *Geophys. Res. Lett.*, **38**, L15810, https://doi.org/10.1029/2011GL048469.

Zhang, J. A., F. D. Marks, J. A. Sippel, R. F. Rogers, X. Zhang, S. G. Gopalakrishnan, Z. Zhang, and V. Tallapragada, 2018: Evaluating the impact of improvement in the horizontal diffusion parameterization on hurricane prediction in the operational Hurricane Weather Research and Forecast (HWRF) Model. *Wea. Forecasting*, **33**, 317–329, https://doi.org/10.1175/WAF-D-17-0097.1.

Zhou, C., H. Shao, and L. Bernardet, 2015: Applications of the GSI-hybrid data assimilation for high-resolution tropical storm forecasts: Tackling the intensity spin-down issue in 2014 HWRF. *16th WRF Users Workshop*, Boulder, CO, Developmental Testbed Center, https://dtcenter.ucar.edu/eval/data_assim/publications/GSI-Hybrid%20at%202015%20WRFUsersWorkshop.v2_poster.pdf.

Zhu, P., B. Tyner, J. A. Zhang, E. Aligo, S. Gopalakrishnan, and D. Frank, 2019: Role of eyewall and rainband eddy forcing in tropical cyclone intensification. *Atmos. Chem. Phys.*, **19**, 14 289–14 310, https://doi.org/10.5194/acp-19-14289-2019.

Zhu, Y., R. Todling, J. Guo, S. E. Cohn, I. M. Navon, and Y. Yang, 2003: The GEOS-3 retrospective data assimilation system: The 6-hour lag case. *Mon. Wea. Rev.*, **131**, 2129–2150, https://doi.org/10.1175/1520-0493(2003)131<2129:TGRDAS>2.0.CO;2.

Zuo, H., M. A. Balmaseda, S. Tietsche, K. Mogensen, and M. Mayer, 2019: The ECMWF operational ensemble reanalysis-analysis system for ocean and sea ice: A description of the system and assessment. *Ocean Sci.*, **15**, 779–808, https://doi.org/10.5194/os-15-779-2019.